

Enhancement of the London penetration depth in pnictides at the onset of SDW order under superconducting dome

A. Levchenko,¹ M. G. Vavilov,² M. Khodas,³ and A. V. Chubukov²

¹*Department of Physics and Astronomy, Michigan State University, East Lansing, Michigan 48824, USA*

²*Department of Physics, University of Wisconsin, Madison, Wisconsin 53706, USA*

³*Department of Physics and Astronomy, University of Iowa, Iowa City, Iowa 52242, USA*

(Dated: April 25, 2013)

Recent measurements of the doping dependence of the London penetration depth $\lambda(x)$ at low T in clean samples of isovalent $\text{BaFe}_2(\text{As}_{1-x}\text{P}_x)_2$ at $T \ll T_c$ [Hashimoto *et al.*, Science **336**, 1554 (2012)] revealed a peak in $\lambda(x)$ near optimal doping $x = 0.3$. The observation of the peak at $T \ll T_c$, points to the existence of the quantum critical point (QCP) beneath the superconducting dome. We associate such a QCP with the onset of a spin-density-wave order and show that the renormalization of $\lambda(x)$ by critical magnetic fluctuations gives rise to the observed feature. We argue that the case of pnictides is conceptually different from a one-component Galilean invariant Fermi liquid, for which correlation effects do not cause the renormalization of the London penetration depth at $T = 0$.

PACS numbers: 74.70.Xa, 74.40.Kb, 74.25.Bt, 74.25.Dw

Introduction.— The properties of iron-based superconductors (FeSCs) have been at the forefront of research activities in the correlated electron community over the last few years [1–4]. These materials have multiple Fermi pockets with electronlike and holelike dispersion of carriers. It is well established that superconductivity in FeSCs emerges in close proximity to a spin-density-wave (SDW) order, and the superconducting (SC) critical temperature T_c has dome-shaped dependence on doping, with T_c maximum near the onset of SDW order [5–8].

Several groups [9] put forward the scenario that superconductivity in FeSCs has s^{+-} symmetry and emerges because SDW fluctuations increase interpocket interaction, which is attractive for s^{+-} gap symmetry, to a level when it overcomes intrapocket repulsion. Likewise, SC fluctuations tend to increase the tendency towards SDW.

Once the system develops long-range order, the situation changes because SDW and SC orders compete, and the order which sets first tends to block the development of the other. According to theory, such competition may give rise to a homogeneous coexistence of SDW and SC orders in some range of dopings [12–14]. A homogeneous coexistence of SDW and SC orders has been detected in 122 materials – electron-doped $\text{Ba}(\text{Fe}_{1-x}\text{Co}_x)_2\text{As}_2$ [7, 8, 15–20] and hole-doped $\text{Ba}_{1-x}\text{K}_x\text{Fe}_2\text{As}_2$ [21–23]. On the other hand, for $\text{EuFe}_{2-x}\text{Co}_x\text{As}_2$ Mössbauer spectroscopy measurements [24] were interpreted in favor of phase separation, when SC has a filamentary character and is concentrated in nonmagnetic regions. In the third class of 122 materials – an isovalent $\text{BaFe}_2(\text{As}_{1-x}\text{P}_x)_2$, the coexistence between SDW and SC order has not yet been probed experimentally, but the odds are that the two orders do coexist because the phase diagram of $\text{BaFe}_2(\text{As}_{1-x}\text{P}_x)_2$ is quite similar to that for $\text{Ba}(\text{Fe}_{1-x}\text{Co}_x)_2\text{As}_2$ [25].

The coexistence implies that the SDW transition line extends into the superconducting phase. If this line reaches $T = 0$, the system develops a magnetic quantum-critical point (QCP) beneath the superconducting dome [11], see Fig. 1. A magnetic QCP without superconductivity has been analyzed in great detail [27, 28], and it is known that quantum fluctuations near this point give rise to non-Fermi liquid (NFL) behavior and to singularities in various electronic characteristics. An SDW instability inside the d -wave SC state has been analyzed in [29] and was shown to give rise to NFL behavior of nodal fermions.

The observation of coexistence brings about the new issue of whether there are electronic singularities at a magnetic QCP which develops in the presence of an s^{+-} SC order. Of particular interest are the singularities in quantities such as the penetration depth $\lambda(x)$, which measures electronic response averaged over the whole Fermi surface (FS). Early experiments [30] on $\text{Ba}(\text{Fe}_{1-x}\text{Co}_x)_2\text{As}_2$ found no special features in $\lambda(x)$ at the onset of SDW order, but recent measurements in $\text{BaFe}_2(\text{As}_{1-x}\text{P}_x)_2$ (Ref. 26) found a peak in $\lambda(x)$ at the smallest $T \ll T_c$ at around optimal doping (see inset of Fig. 1). The authors of Ref. [26] speculated that the peak likely indicates that there is a QCP beneath a SC dome and argued that the peak in $\lambda(x)$ is a generic feature of 122 Fe pnictides, but it is more difficult to detect it in $\text{Ba}(\text{Fe}_{1-x}\text{Co}_x)_2\text{As}_2$ because of the greater degree of electronic disorder caused by Co doping. Another potential reason why the peak has been observed only in $\text{BaFe}_2(\text{As}_{1-x}\text{P}_x)_2$ is that this material possesses gap nodes [31], which generally lead to stronger effects due to quantum fluctuations.

In this Letter, we analyze the behavior of $\lambda(x)$ under the assumption that the QCP is associated with the development of SDW order beneath a superconducting dome. A preemptive nematic order may also play a role [32], but we will not dwell on that.

London penetration depth near QCP. – In general, the peak in $\lambda(x)$ at a SDW QCP can emerge for one of three

reasons: (i) a nonmonotonic behavior of λ near a QCP already within the mean-field theory (like the peak in the specific heat jump at T_c at the onset of coexistence with SDW [33]), (ii) critical fluctuations at the onset of SDW, not specific to the form of the gap, and (iii) critical fluctuations specific to the presence of the gap nodes. Besides, λ can either diverge at a QCP, or get enhanced but stay finite. It was found recently [34] that, at the mean field level, the variation of λ is smooth and cannot explain sharp features observed in Ref. [26]. Here, we investigate the effects of critical magnetic fluctuations. We find that fluctuations associated with SDW QCP beneath a SC dome give rise to the enhancement of the effective mass m^* . The mass does not diverge because SC order cuts infrared singularities, but, nevertheless, m^*/m at the QCP is noticeably enhanced. We argue that the enhancement of m^* gives rise to a sharp peak in $\lambda(x)$ at the onset of coexistence with SDW. We also find that the presence of the nodes in the gap is not sufficient to transform a peak into a divergence because the dominant contribution to m^* comes from the region away from the nodes.

London penetration depth in a type-II superconductor with cubic symmetry is expressed via the zero-momentum component of the electromagnetic response tensor $Q_{ij}(\mathbf{k}) = (\delta_{ij} - k_i k_j / k^2) Q(\mathbf{k})$, which relates vector potential \mathbf{A} and the current density \mathbf{j} : $j_i(\mathbf{k}) = -Q_{ij}(\mathbf{k}) A_j(\mathbf{k})$. The temperature and doping dependent penetration depth is given by $\lambda^{-2}(T, x) = (4\pi/c) Q(T, x)$, where c is the velocity of light. The kernel $Q(T, x)$ is related to the current-current correlation function in the limit of zero frequency and vanishing momentum and is expressed via the superfluid density $n_s(T, x)$ as $Q = e^2 n_s / mc$, where m and e are the mass and the charge of an electron. Then $\lambda^2 = mc^2 / (4\pi e^2 n_s)$. In the Galilean invariant, a one-component fermionic system superfluid density at $T = 0$ is equal to the total density of fermions $n(x)$. In this situation, $\lambda(T = 0, x)$ does not depend on Fermi liquid corrections and remains the same as in a Fermi gas [35, 36]. Diagrammatically, superfluid density is given by the sum of two bubble diagrams made out of normal and anomalous Green's functions, and the independence of $n_s(T = 0, x)$ on the electron-electron interaction is the result of the cancelation between self-energy and vertex corrections to these diagrams. At $T > 0$ the T -dependent part of n_s does depend on Fermi liquid parameters [36].

We find, however, that in iron pnictides the situation is different because these systems have multiple Fermi pockets, and s^{+-} pairing originating from inter-pocket interaction. The interplay between self-energy and vertex corrections then depends on the orientation of Fermi velocities and the values of superconducting order parameters at different FSs. We find that self-energy and vertex corrections generally do not cancel, and the penetration depth is roughly proportional to m^*/m .

We followed earlier works [9] and assumed that the most relevant interaction in Fe pnictides is between hole and electron pockets, separated by $\mathbf{Q} = (\pi, \pi)$ in the folded Brillouin zone, and that the gap has s^{+-} symmetry and changes sign between electron and hole pockets. We calculated the leading interaction correction to $\lambda(x)$ in the one-loop approximation. This perturbative analysis is justified because renormalized $\lambda(x)$ does not diverge even at a SDW QCP. There are 16 diagrams with one-loop corrections to current-current correlators, half of them are self-energy and half are vertex corrections. We evaluated the diagrams and found that self-energy and vertex corrections are of the same order, and both decrease the superfluid density and increase the penetration depth [37]. To be brief, below we analyze how $\lambda(x)$ is affected by inserting fermionic self-energy into the current correlation function. A straightforward calculation yields, at one-loop order

$$\lambda^2(T = 0, x) = \lambda_{BCS}^2 [1 + \beta(x)], \quad (1)$$

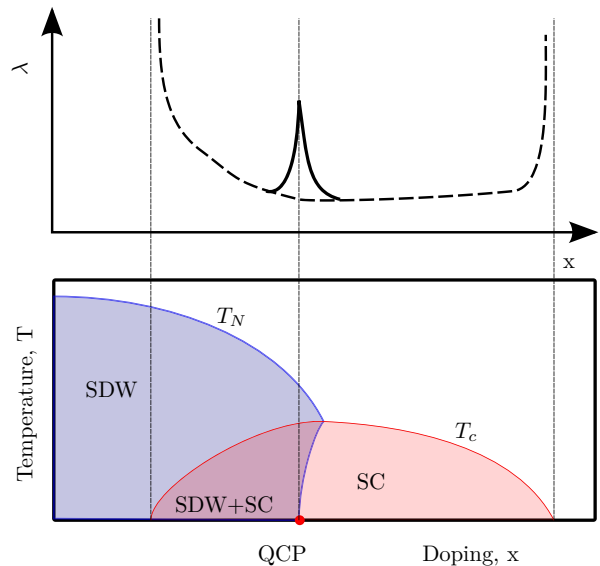


FIG. 1: Lower panel: a theoretical phase diagram of 122-type iron-based superconductors in temperature *vs* doping planes. Critical temperatures T_N and T_c indicate transitions into pure SDW and SC phases, respectively. A QCP lies beneath the SC dome and separates pure SC and coexistence SC+SDW phases. Reentrant behavior of T_N under the SC dome has been detected in Co-doped 122 materials [10] but well may be nonuniversal [11–14]. Upper panel: the theoretical behavior of the penetration depth λ at $T = 0$. In the mean-field approximation (dashed line), λ diverges at the edges of the superconducting dome, flat inside pure SC phase and increases monotonically as the system moves towards the pure SDW phase. Beyond the mean field, magnetic fluctuations give rise to a peak in λ at the onset of the SDW order (solid line). The peak in λ has been observed in Ref. [26].

where

$$\beta = \left\langle \sum_j [1 - Z_j(\mathbf{k}_F)] \right\rangle_\phi = \left\langle \lim_{\omega \rightarrow 0} \partial_{i\omega_m} \Sigma_j(\mathbf{k}_F, \omega_m) \right\rangle_\phi. \quad (2)$$

Here, j labels Fermi pockets, Σ is a diagonal (normal) self-energy, which generally depends on the location of \mathbf{k}_F on the corresponding Fermi surface, and $\langle \dots \rangle_\phi = \int_0^{2\pi} \dots d\phi / 2\pi$. In a situation where the dependence of $\Sigma_j(\mathbf{k}, \omega_m)$ on $\mathbf{k} - \mathbf{k}_F$ can be neglected, the quasiparticle residue is related to mass renormalization as $Z_j(\mathbf{k}_F) = m/m_j^*(\mathbf{k}_F)$.

A similar expression for λ has been obtained earlier for heavy-fermion superconductor UBe₁₃ [38], which is a two-component system of conduction d -electrons and localized f electrons, of which only the first carry the current. It is tempting to extend the one-loop result (1) to $\lambda^{-2} \propto \sum_j m/m_j^*$, but we caution that noncancellation of one-loop self-energy and vertex corrections to the current correlator does not necessarily imply that vertex corrections can be simply neglected. An example of more complex behavior beyond one-loop order has been recently considered in [39].

Evaluation of the fermionic self-energy.— We consider the minimal three-band model of two elliptical electron Fermi surfaces and one circular hole Fermi surface. The basic Hamiltonian includes the free fermion part H_0 and pair fermion interactions in superconducting H_Δ and magnetic H_σ channels [37]. These interactions are described by the local coupling constants g_{sc} and g_{sdw} respectively. The phase diagram of the model has been obtained before [14]. We focus on the region where at $T = 0$ the system has a long-range SC order and is about to develop an SDW order. Renormalization of mass on all Fermi surfaces is of the same order, and for brevity we show the calculations of m^*/m for just one pocket.

Potentially, singular self-energy comes from the exchange of near-critical SDW fluctuations. In the normal state, these fluctuations are overdamped and are slow compared to electrons. In a SC state, the dynamical exponent changes from $z = 2$ to $z = 1$ because fermions which contribute to bosonic dynamics become massive particlelike excitations. Such systems have been discussed earlier in the context of cuprates [27] and we follow the same approach in deriving the expressions for the self-energy and spin polarization operator in the SC state in our case.

The one-loop self-energy due to spin-fluctuation exchange is a convolution of spin-fluctuation and fermionic propagators, both taken in the superconducting state:

$$\Sigma_j(\mathbf{k}, \omega_n) = 3T \sum_{\Omega_m} \int \frac{d\mathbf{q}}{4\pi^2} L(\mathbf{q}, \Omega_m) \mathcal{G}_j(\mathbf{k} - \mathbf{q}, \omega_n - \Omega_m) \quad (3)$$

where $\omega_m = 2\pi T(n + 1/2)$ and $\Omega_m = 2\pi mT$ are fermionic and bosonic Matsubara frequencies respectively. The normal and anomalous components of the Green's function in the SC are

$$\mathcal{G}_j(\mathbf{k}, \omega_n) = \frac{-i\omega_n - \xi_j}{\xi_j^2 + \omega_n^2 + \Delta_j^2}, \quad \mathcal{F}_j(\mathbf{k}, \omega_n) = \frac{-\Delta_j}{\xi_j^2 + \omega_n^2 + \Delta_j^2} \quad (4)$$

where $\xi_j = \xi_j(\mathbf{k}) = \mathbf{v}_{j,F}(\mathbf{k} - \mathbf{k}_F)$, and the energy gap Δ_j is equal to Δ_h on the hole Fermi surfaces and $\Delta_e(\phi) = -\Delta_e(1 \pm \alpha \cos 2\phi)$ on the two electron Fermi surfaces (we choose $\Delta_h, \Delta_e > 0$). The gaps on electron pockets have nodes when $\alpha > 1$. We emphasize that the SC gap can be treated as doping independent only in the paramagnetic state. Once SDW order sets in, the value of the gap changes [12–14].

The spin-fluctuation propagator is given by

$$L(\mathbf{q}, \Omega_m) = \frac{1}{g_{sdw}^{-1} + \Pi(\mathbf{q}, \Omega_m)}, \quad (5)$$

where the polarization operator $\Pi(\mathbf{q}, \Omega_m)$ is (see [37] for details)

$$\Pi = N_f T \sum_{\omega_n} \int d\xi \left\langle \frac{[i\omega_+ - \xi_+][i\omega_- + \xi_-] + \Delta_h \Delta_e}{[\xi_+^2 + \omega_+^2 + \Delta_h^2][\xi_-^2 + \omega_-^2 + \Delta_e^2]} \right\rangle_\phi. \quad (6)$$

Here $\omega_\pm = \omega_n \pm \Omega_m/2$, $\xi_\pm = \xi \pm \delta/2$, and we replaced the integration over momentum \mathbf{k} by $\int \dots d^2\mathbf{k}/4\pi^2 = N_f \int \dots d\xi d\phi/(2\pi)$, where N_f is the density of states. Parameter $\delta = \delta_\phi + \delta_q$ accounts for the doping-induced modification of the Fermi surfaces. The term $\delta_\phi = \delta_0 + \delta_2 \cos 2\phi$ describes changes in the Fermi surfaces radii and overall shape (ellipticity), while the term $\delta_q = v_F q \cos(\phi - \psi)$ describes the relative shift in the centers of Fermi surfaces, where ϕ and ψ are the directions of \mathbf{k}_F and \mathbf{q} . The magnetic SDW critical point is determined in terms of doping parameters δ_0 and δ_2 from the condition $\Gamma = 0$, where $\Gamma = (g_{sdw}^{-1} + \Pi(0, 0))N_f^{-1}$.

We first consider the case of equal gaps on both Fermi surfaces ($\alpha = 0$, $\Delta_h = \Delta_e = \Delta$) and then discuss how the results are modified in the case where the gaps on electron pockets have nodes. Earlier calculations show [13] that there is a broad parameter range $0.8 \lesssim \delta_2/\delta_0 \lesssim 4.7$ for which SDW order emerges gradually, and its appearance does not destroy SC order; i.e., SDW and SC orders coexist over some range of dopings. Since we are interested in the $T = 0$ limit, it is sufficient to evaluate the propagator of magnetic fluctuations in Eq. (5) only at small frequencies and momenta. A straightforward expansion leads to [37]

$$L(\mathbf{q}, \Omega_m) = \frac{1}{N_f} \frac{1}{\eta v_F^2 q^2 + \chi \Omega_m^2 + \Gamma}, \quad (7)$$

where

$$\Gamma = \ln \left(\frac{T_{c,0}}{T_{N,0}} \right) - \left\langle \frac{|\delta_\phi| \operatorname{arccosh} \sqrt{1 + \delta_\phi^2/\Delta^2}}{\sqrt{\delta_\phi^2 + \Delta^2}} \right\rangle_\phi, \quad (8a)$$

$$\chi(\Delta, \delta) = \frac{1}{8} \left\langle \frac{1}{\Delta^2 + \delta_\phi^2} + \frac{\Delta^2 \operatorname{arccosh} \left(\sqrt{1 + \delta_\phi^2/\Delta^2} \right)}{|\delta_\phi| (\Delta^2 + \delta_\phi^2)^{3/2}} \right\rangle_\phi, \quad (8b)$$

and

$$\eta(\Delta, \delta, \psi) = \frac{1}{8} \left\langle \cos^2(\phi - \psi) \left[\frac{2\Delta^2 - \delta_\phi^2}{(\Delta^2 + \delta_\phi^2)^2} - 3\Delta^2 |\delta_\phi| \frac{\operatorname{arccosh} \left(\sqrt{1 + \delta_\phi^2/\Delta^2} \right)}{(\Delta^2 + \delta_\phi^2)^{5/2}} \right] \right\rangle_\phi. \quad (8c)$$

In Eq. (8a), we absorbed coupling constants g_{sdw} (g_{sc}) into the corresponding critical temperatures $T_{N,0}$ ($T_{c,0}$) for the transitions into a pure SDW (SC) state.

Without superconductivity, $\eta < 0$, and a magnetic transition at $T = 0$ is into an incommensurate phase [14, 32]. In the presence of SC order, the commensurate (π, π) magnetic order is stabilized ($\eta > 0$), provided that relevant $\delta_\phi^2 \leq \Delta^2$, which we assume to hold. By order of magnitude, $\chi \sim \eta \sim 1/\Delta^2$.

Substituting Eqs. (4) and (7) into Eq. (2) and integrating explicitly over the momentum transfer \mathbf{q} (see Supplementary material for details), we obtain the fermionic residue for a direction ϕ along the Fermi surface in the form $Z(\phi) = 1 - I(\phi)F$. Here $I(\phi)$ accounts for the (nonsingular) angular dependence and is normalized such that $(\phi_h) = 1$, where ϕ_h is the direction of a hot spot (a \mathbf{k}_F point for which $\mathbf{k}_F + \mathbf{Q}$ is also on another Fermi surface, see Fig. 2(a), and F accounts for the dependence on the distance to the hot spot, measured by Γ , and on the system parameters δ_0 and δ_2 . In explicit form $F = \langle F(\kappa(\psi), \gamma(\psi)) \rangle_\psi$, where $\kappa(\psi) = \chi/\eta(\psi)$, $\gamma = \Gamma/\eta(\psi)\Delta^2$, and

$$F(\kappa, \gamma) = \frac{3}{8\pi^2 \eta N_f v_F^2 \Delta} \int_{-\infty}^{+\infty} \frac{\kappa z^2 dz}{(1 - \kappa)z^2 + 1 - \gamma} \times \left[\frac{1}{\kappa z^2 + \gamma} - \frac{\operatorname{arccosh} \left(\sqrt{\frac{z^2 + 1}{\kappa z^2 + \gamma}} \right)}{\sqrt{z^2 + 1} \sqrt{(1 - \kappa)z^2 + 1 - \gamma}} \right]. \quad (9)$$

Using Eqs. (1) and (2) we find

$$\beta = \lambda^2/\lambda_{BCS}^2 - 1 = F\langle I(\phi) \rangle \quad (10)$$

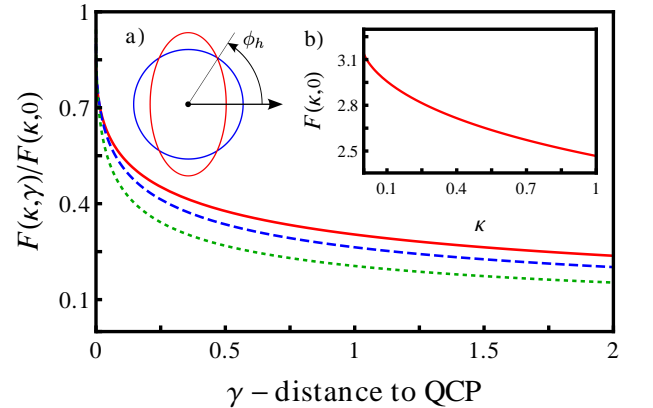


FIG. 2: Scaling function $F(\kappa, \gamma)$ which accounts for the interaction correction to the London penetration depth $\lambda^2/\lambda_{BCS}^2 - 1 \propto F(\kappa, \gamma)$ is plotted vs γ which measures the distance to the quantum critical point for three different combinations of the system parameters encoded by $\kappa = 0.1, 0.25, 0.5$. (see text). Insets: (a) hole (circular) and electron (elliptical) Fermi surfaces, ϕ_h marks the location of a hot spot; (b) the dependence of $F(\kappa, 0)$, normalized to the prefactor in Eq. 9, on κ .

Because angular integrals over ϕ in $I(\phi)$ and over ψ in F are nonsingular, the dependence of β on the distance to the critical point and on system parameters can be approximated by $\beta \sim F(\kappa, \gamma)$. It is apparent from the integral in (9) that $F(\kappa, \gamma)$ is finite even in the limit $\gamma \rightarrow 0$, which implies that the penetration depth remains finite at the SDW QCP. Still, $F(\kappa, \gamma)$ is peaked at the SDW QCP (when $\gamma = 0$), and decreases as $F(\kappa, \gamma) \propto \ln \gamma / \sqrt{\gamma}$ at $\gamma \gg 1$. We illustrate this behavior in Fig. 2. Because $\delta\lambda \sim F(\kappa, \gamma)$, the penetration depth is also peaked at the QCP. This behavior is in agreement with the data for isovalent $\text{BaFe}_2(\text{As}_{1-x}\text{P}_x)_2$ [26].

By order of magnitude $F(\kappa, 0) = O(1)$, hence $\beta = O(1)$. The enhancement of $\lambda^2 = \lambda_{BCS}^2(1 + \beta)$ at the SDW QCP is larger if magnetic order remains commensurate (π, π) even in the absence of superconductivity. In this situation, δ_0 and δ_2 are not restricted to be smaller than Δ , and, if they are larger, β is enhanced by $(\delta/\Delta)^2$. We caution, however, that once β becomes large, the one-loop approximation is no longer applicable, and, in particular, vertex corrections has been analyzed in more detail [39].

We next computed $F(\kappa, \gamma)$ for the case when the SC gap has nodes on electron pockets. We found that, roughly, the angular dependence of the gap renormalizes κ downward. This, however, does not change λ qualitatively – at a magnetic QCP $F(\kappa, 0)$ increases when κ decreases, but still remains finite. We illustrate this in Fig. 2(b). The reasoning is simple: the nodes of the s^{+-} gap are located at accidental \mathbf{k}_F points which generally differ from hot spots. In the special case where the gap nodes coincide with hot spots, Z at a hot spot diverges logarithmically at a SDW QCP, but the momentum integral of $Z(\phi)$ is still finite, hence, λ remains finite even in this case.

Conclusions.– In this Letter we considered the behavior of the penetration depth $\lambda(x)$ in a clean Fe-based s^{+-} superconductor at the onset of a commensurate SDW order inside the SC phase at $T = 0$. We found that the penetration depth remains finite but has a peak at the onset of SDW order. The magnitude of the peak is larger when the s^{+-} gap has accidental nodes, but still remains finite at the onset of SDW order. Our results agree with the measurements [26] of the penetration depth in the isovalent $\text{BaFe}_2(\text{As}_{1-x}\text{P}_x)_2$ inside the superconducting phase. Experiment [26] shows that λ has a peak at roughly the same doping where the Néel temperature T_N intersects with T_c . Our results support the scenario that SDW order in $\text{BaFe}_2(\text{As}_{1-x}\text{P}_x)_2$ persists into the SC phase, as happens in other Fe-based superconductors, and that the peak in the penetration depth occurs at a magnetic quantum-critical point inside the SC dome. Whether SDW and SC orders coexist microscopically or phase separate, remains to be seen.

We thank Y. Matsuda, T. Shibauchi, R. Fernandes, S. Maiti, R. Prozorov, and S. Sachdev for useful discussions. A.L. acknowledges support from Michigan State University. M.G.V. is supported by NSF Grant No. DMR 0955500. A.V.C. is supported by the DOE Grant No. DE-FG02-ER46900.

The model Hamiltonian

The basic Hamiltonian for electron-electron interaction includes the free fermion part H_0 , and four-fermion interaction terms. In the orbital basis, the free-electron part contains inter-and inter-orbital hopping terms, and the interaction part contains intra-orbital and inter-orbital density-density interactions (the Hubbard terms U and U'), the spin-spin interaction J (the Hund coupling), and the pair-hopping term J' (Ref.[9, 40]).

The orbital Hamiltonian is converted into band basis by diagonalization of the quadratic form. The new quadratic part describes fermions near hole and electron pockets. We adopt the minimal three-band model with one hole and two electron pockets. In this model

$$H_0 = \sum_{\mathbf{k}s} \xi_h(\mathbf{k}) c_{\mathbf{k}s}^\dagger c_{\mathbf{k}s} + \sum_{\mathbf{k}'sj} \xi_{je}(\mathbf{k}') f_{\mathbf{k}'sj}^\dagger f_{\mathbf{k}'sj} \quad (11)$$

where creation/annihilation c -operators describe fermions near the hole pocket, and f -operators describe fermions near the electron pockets labeled by $j = 1, 2$; ξ_h and ξ_{je} are corresponding dispersions. The momenta \mathbf{k} are measured from the center of the Brillouin zone and \mathbf{k}' are deviations from $\mathbf{Q} = (\pi, \pi)$.

The four-fermion interaction terms in the band basis are Hubbard, Hund, and pair-hopping interactions, dressed by coherence factors from the diagonalization of the quadratic form. There are five different interaction terms in the band basis [41] – two density-density intra-pocket interactions (u_4 and u_5 terms in the notations of [41], these interactions are often treated as equal), density-density inter-pocket interaction u_1 , exchange inter-pocket interaction u_2 , and inter-pocket pair hopping u_3 . These five interactions can be re-absorbed into interactions in the particle-particle channel, and SDW and CDW particle-hole channels. For repulsive interactions, SDW and SC channels are the two most relevant ones. In general, these two interactions may depend on the directions along the pockets.

For spin-single SC channel, the most relevant interaction is the pair hopping of two fermions from electron to hole pockets and vice versa

$$H_{\Delta} = \frac{1}{2} \sum_{\mathbf{k}\mathbf{p}} \sum_{jss'\sigma\sigma'} g_{ss'\sigma\sigma'}^{sc}(\mathbf{k}, \mathbf{p}) [c_{\mathbf{k}s}^{\dagger} c_{-\mathbf{k}\sigma}^{\dagger} f_{-\mathbf{p}\sigma'j} f_{\mathbf{p}s'j} + f_{\mathbf{k}s}^{\dagger} f_{-\mathbf{k}\sigma}^{\dagger} c_{-\mathbf{p}\sigma'} c_{\mathbf{p}s}]. \quad (12)$$

where $g_{ss'\sigma\sigma'}^{sc}(\mathbf{k}, \mathbf{p}) = u_3(i\tau^y)_{s\sigma}(i\tau^y)_{\sigma's'}^{\dagger}$. Once u_3 exceeds intra-pocket density-density interaction u_4 , the system develops a \pm s-wave superconductivity. Since our goal is to analyze the behavior of the penetration depth deep in the superconducting state, we do not explicitly solve superconducting problem, but rather assume that for the doping range we are interested in the system at $T = 0$ is already in the superconducting state.

The magnetic SDW interaction between fermions is [14]

$$H_{\sigma} = -\frac{1}{4} \sum_{\mathbf{p}' - \mathbf{p} = \mathbf{k}' - \mathbf{k}} \sum_{jss'\sigma\sigma'} g_{ss'\sigma\sigma'}^{sdw}(\mathbf{p}\mathbf{p}', \mathbf{k}\mathbf{k}') [f_{\mathbf{p}'s'j}^{\dagger} c_{\mathbf{p}\sigma}^{\dagger} c_{\mathbf{k}\sigma'}^{\dagger} f_{\mathbf{k}'s'j} + f_{-\mathbf{p}'s'j}^{\dagger} c_{-\mathbf{p}\sigma}^{\dagger} c_{-\mathbf{k}\sigma'}^{\dagger} f_{-\mathbf{k}'s'j}]. \quad (13)$$

where $g_{ss'\sigma\sigma'}^{sdw}(\mathbf{p}\mathbf{p}', \mathbf{k}\mathbf{k}') = (u_1 + u_3)\tau_{s\sigma} \cdot \tau_{\sigma's'}^{\dagger}$, and τ are the Pauli matrices.

This is the bare interaction in the SDW channel. The full one is obtained by dressing this interaction by RPA-type bubbles [9]a. Such a renormalization (described in detail in [40]) transforms a constant interaction into an effective interaction mediated by collective spin fluctuations. The static part of the spin-fluctuation propagator comes from high-energy fermions, is regular, and can be absorbed into g_{sdw} . The dynamical part of the spin-polarization operator comes from fermions with low-energies [42] and has to be treated exactly. This last renormalization is given by the sum of bubbles made of normal and anomalous fermionic Green functions in a superconductor. In explicit form, the spin-fluctuation propagator is given by Eqs. (5) and (6) in the main text.

Derivation of Γ in Eq. (8a)

Distance to the quantum critical point in our model is defined by $\Gamma = (g_{sdw}^{-1} - \Pi(0, 0))/N_f$, where $\Pi(\mathbf{q}, \Omega)$ is the polarization operator. Here we provide the details of the derivation of the equation for Γ [Eq. (8a) in the main text]. From Eq. (6) of the main text, we have:

$$\Pi(0, 0) = -2\pi T N_f \sum_{\omega_n > 0} \left\langle \frac{E_n}{E_n^2 + \delta_{\phi}^2} \right\rangle_{\phi}, \quad E_n^2 = \omega_n^2 + \Delta^2. \quad (14)$$

where $\langle \dots \rangle_{\phi} = \int_0^{2\pi} \dots d\phi / 2\pi$. Hence

$$\Gamma = \frac{1}{g_{sdw} N_f} - 2\pi T \sum_{\omega_n > 0} \left\langle \frac{E_n}{E_n^2 + \delta_{\phi}^2} \right\rangle_{\phi}. \quad (15)$$

The coupling constant g_{sdw} can be eliminated in favor of the transition temperature into the pure SDW state, $T_{s,0} = (2e^{\gamma_E}/\pi)\Lambda \exp(-1/g_{sdw}N_f)$, which allows us to rewrite the equation above as

$$\Gamma = \ln \left(\frac{T}{T_{s,0}} \right) - 2\pi T \sum_{\omega_n > 0} \left\langle \frac{E_n}{E_n^2 + \delta_{\phi}^2} - \frac{1}{\omega_n} \right\rangle_{\phi}. \quad (16)$$

Next we add and subtract $1/E_n$ inside the angle brackets and take the zero temperature limit. The infrared convergent part of the Matsubara sum can be safely converted into the frequency integral, while infra-red divergent part is evaluated using $2\pi T \sum_{\omega_n} [1/E_n - 1/\omega_n] = \ln(\pi e^{-\gamma_E} T / \Delta)$. This yields

$$\Gamma = \ln \left(\frac{T}{T_{s,0}} \right) + \left\langle \int_0^{\infty} d\omega \frac{\delta_{\phi}^2}{\sqrt{\omega^2 + \Delta^2}(\omega^2 + \Delta^2 + \delta_{\phi}^2)} \right\rangle_{\phi} - \ln \left(\frac{\pi e^{-\gamma_E} T}{\Delta} \right). \quad (17)$$

Combining two logarithmic terms and using BCS expression between the gap and critical temperature $\Delta = \pi e^{-\gamma_E} T_{c,0}$ one finds for their difference $\ln(T_{c,0}/T_{s,0})$. The remaining energy integral can be computed analytically with the help of the formula

$$\int_0^{\infty} \frac{dx}{\sqrt{x^2 + a^2}(x^2 + b^2)} = \frac{\text{arccosh}(b/a)}{|b|\sqrt{b^2 - a^2}}. \quad (18)$$

Combining last two expressions, we reproduce Eq. (8a) of the main text.

Expansion of the polarization operator $\Pi(\mathbf{q}, \Omega_m)$

To obtain Eq. (7) of the main text, we need to expand the polarization operator $\Pi(\mathbf{q}, \Omega)$ to order q^2 and Ω^2 . Expanding the integrand in Eq. (6) of the main text and integrating over ξ we obtain

$$\Pi(\mathbf{q}, \Omega_m) = \Pi(0, 0) + \delta\Pi(0, \Omega_m) + \delta\Pi(\mathbf{q}, 0), \quad (19)$$

$$\delta\Pi(0, \Omega_m) = \frac{1}{16} N_f T \Delta^2 \Omega_m^2 \sum_{\omega_n} \int d\phi \frac{\delta_\phi^2 + 3(\Delta^2 + \omega_n^2)}{(\omega_n^2 + \Delta^2)^{3/2} (\omega_n^2 + \Delta^2 + \delta_\phi^2)^2}, \quad (20)$$

$$\delta\Pi(\mathbf{q}, 0) = \frac{1}{8} N_f T (v_F q)^2 \sum_{\omega_n} \int d\phi \frac{\sqrt{\Delta^2 + \omega_n^2} (-3\delta_\phi^2 + \Delta^2 + \omega_n^2)}{(\omega_n^2 + \delta_\phi^2 + \Delta^2)^3}. \quad (21)$$

At $T \rightarrow 0$, Matsubara sums over ω_m can be converted into frequency integrals. Integrating over ω_m , we reproduce Eqs. (7), (8b) and (8c) of the main text.

Calculation of the self-energy diagram

To calculate λ/λ_{BCS} , we need to know $1 - Z(\mathbf{k}_F) = \lim_{\omega \rightarrow 0} \partial_{i\omega} \Sigma_j(\mathbf{k}_F, \omega_m)$. The self-energy is introduced in Eq. (4) of the main text. We have

$$1 - Z(\mathbf{k}_F) = 3T \lim_{\omega \rightarrow 0} \sum_{\mathbf{q}, \Omega} L(\mathbf{q}, \Omega) \frac{\partial \mathcal{G}(\mathbf{k}_F - \mathbf{q}, \omega - \Omega)}{\partial(i\omega)} \quad (22)$$

Using $\partial_{i\omega} = -\partial_{i\Omega}$, taking the limit $\omega \rightarrow 0$, and integrating by parts, we obtain

$$1 - Z(\mathbf{k}_F) = 3T \sum_{\mathbf{q}, \Omega} \frac{\partial L(\mathbf{q}, \Omega)}{\partial(i\Omega)} \mathcal{G}(\mathbf{k}_F - \mathbf{q}, -\Omega) \quad (23)$$

Let's first focus on \mathbf{k}_F at a hot spot. Using the explicit forms of the SC Green's function from Eq. (4) and SDW fluctuation propagator from Eq. (7), we express the quasi-particle residue as

$$1 - Z(\mathbf{k}_F) = \frac{6\chi T}{N_f} \sum_{\mathbf{q}, \Omega} \frac{\Omega^2}{(\eta v_F^2 q^2 + \chi \Omega^2 + \Gamma)^2 (v_F^2 q_x^2 + \Omega^2 + \Delta^2)} \quad (24)$$

The position of \mathbf{k}_F on the Fermi surface is specified by the angle ϕ , χ and Γ are given by Eqs. (8a) and (8b) in the main text and depend on system parameters, and η is given by Eqn. (8c) and depends on system parameters and on the direction of \mathbf{q} set by angle ψ (i.e., $\eta = \eta(\psi)$). Taking the limit of zero temperature and introducing dimensionless variables

$$x = \frac{v_F q_x}{\Delta} \quad y = \frac{v_F q_y}{\Delta} \quad z = \frac{\Omega}{\Delta} \quad \gamma(\psi) = \frac{\Gamma}{\eta(\psi) \Delta^2} \quad \kappa(\psi) = \frac{\chi}{\eta(\psi)}, \quad (25)$$

we re-express Eq. (24) as

$$1 - Z(\mathbf{k}_F) = \langle F(\kappa(\psi), \gamma(\psi)) \rangle_\psi \quad (26)$$

where

$$F(\kappa, \gamma) = \frac{3\kappa}{4\pi^3 \eta N_f v_F^2 \Delta} \iiint_{-\infty}^{+\infty} \frac{z^2 dx dy dz}{(x^2 + y^2 + \kappa z^2 + \gamma)^2 (x^2 + z^2 + 1)}. \quad (27)$$

Integrating over y and then over x , we obtain Eq. (9) of the main text.

When \mathbf{k}_F is not at the hot spot, the expression for the self-energy becomes more complex, because an intermediate fermion at $\mathbf{k}_F + \mathbf{Q}$ is no longer located at the Fermi surface. This reduces the self-energy compared to its value at a hot spot. Roughly, Δ in Eq. (24) get replaced by $\sqrt{\Delta^2 + v_F^2 k_F^2(\phi)}$, where $k_F(\phi)$ is the deviation from a hot spot along the corresponding Fermi surface. With this modification, $1 - Z(\mathbf{k}_F)$ acquires an extra factor $I(\phi) \approx 1/\sqrt{1 + (k_F(\phi)/k_0)^2}$,

where $k_0 = \Delta/v_F$. At a hot spot, $\phi = \phi_h$ and $I(\phi_h) = 1$. The parameter γ also has to be modified accordingly, but this is not important for our purposes because we treat γ as a phenomenological parameter which measures the distance to a magnetic critical point.

It is instructive to analyze in more detail $F(\kappa, \gamma)$ at the SDW QCP, when $\gamma = 0$. We have

$$F(\kappa, 0) = \frac{3}{8\pi^2\eta N_f v_F^2 \Delta} \int_{-\infty}^{+\infty} \frac{\kappa z^2 dz}{(1-\kappa)z^2 + 1} \left[\frac{1}{\kappa z^2} - \frac{\text{arccosh}\left(\frac{\sqrt{z^2+1}}{\sqrt{\kappa}|z|}\right)}{\sqrt{z^2+1}\sqrt{(1-\kappa)z^2+1}} \right]. \quad (28)$$

One can easily make sure that at $\kappa \ll 1$, the dominant contribution to the integral comes from small $z \sim \kappa$. For such z , $\text{arccosh}(\sqrt{z^2+1}/\sqrt{\kappa}|z|) \approx \ln(2/\sqrt{\kappa}|z|)$, and hence

$$F(\kappa, 0) \approx \frac{3}{8\pi^2\eta N_f v_F^2 \Delta} \int_{-\infty}^{+\infty} \left[\frac{1}{1+z^2} - \frac{\kappa z^2 \ln\left(\frac{1}{\sqrt{\kappa}|z|}\right)}{(z^2+1)^2} \right] dz. \quad (29)$$

With the logarithmic accuracy this yields

$$F(\kappa, 0) \approx \frac{3}{8\pi\eta N_f v_F^2 \Delta} \left[1 - \frac{\kappa}{4} \ln\left(\frac{1}{\kappa}\right) \right], \quad \kappa \ll 1. \quad (30)$$

In the opposite limit $\kappa \gg 1$ the integral predominantly comes from $z \sim 1/\sqrt{\kappa}$, and we have

$$F(\kappa, 0) \approx \frac{1}{12\pi^2\eta N_f v_F^2 \Delta} \frac{\ln \kappa}{\sqrt{\kappa}}, \quad \kappa \gg 1. \quad (31)$$

Interplay between self-energy and vertex corrections to the current correlation function

In this section we present calculations to prove the point in the main text that one loop self-energy and vertex corrections to current correlation function in a superconducting state of an Fe-pnictide add up rather than cancel. We argue that non-cancellation is the consequence of the fact that the system lacks Galilean invariance (electron pockets are located at the corners of the Brillouin zone), and it holds even if the dispersion within each band can be approximated by a quadratic one. We contrast Fe-pnictides to single-band superconductors with the quadratic dispersion. In the latter vertex and self-energy corrections cancel out, as required by Galilean invariance [35, 36, 43]. To emphasize this point, we assume that the electronic dispersion near hole and electron pockets is quadratic and consider two cases – only intra-pocket interaction and only inter-pocket interaction. The first case models Galilean invariant case (hole and electron pockets do not couple), the second case models s^{+-} superconductivity in Fe-pnictides (hole and electron pockets are coupled, and the superconducting gaps on the two are determined self-consistently).

We compute the interaction correction to the function $Q(\vec{k})$ introduced in the main text. In the London limit, $Q(\vec{k} \rightarrow 0) = Q = -c^{-1} \int_0^{T^{-1}} d\tau \int d\vec{x} \langle j_x(\tau) j_x(0) \rangle$, where $\vec{j} = e \sum_{\vec{p}, \alpha} \psi_{\vec{p}, \alpha}^\dagger \vec{v}_{\vec{p}} \psi_{\vec{p}, \alpha}$, and $\alpha = 1, 2$ accounts for spin projections. The penetration depth is related to Q as $\lambda^{-2} = (4\pi/c)Q$.

In the non-interacting case, $Q = Q_0$ is given by the two bubble diagrams made of the normal and anomalous Green's function, Fig. 3. At $T = 0$ we have

$$Q_0 = \lim_{\vec{k} \rightarrow 0} \frac{2e^2}{c} \frac{N_F}{d} \int d\xi \int \frac{d\omega}{2\pi} \int \frac{d\theta}{2\pi} \{ v_{x, \vec{p}}^2 [\mathcal{G}(\xi_+, \omega) \mathcal{G}(\xi_-, \omega) + \mathcal{F}(\xi_+, \omega) \mathcal{F}(\xi_-, \omega) - \mathcal{G}_n(\xi_+, \omega) \mathcal{G}_n(\xi_-, \omega)] \}, \quad (32)$$

where $\xi_{\pm} = \xi \pm \vec{v}_{\vec{p}} \vec{k}/2$, the overall factor of 2 is due to spin summation, d is the inter-layer spacing, $N_F = m/(2\pi)$ is the 2D density of states, and the normal and anomalous Green's functions \mathcal{G} and \mathcal{F} are

$$\mathcal{G}(\xi_{\vec{p}}, \omega_n) = -\frac{i\omega_n + \xi_{\vec{p}}}{\omega_n^2 + \xi_{\vec{p}}^2 + \Delta^2}, \quad \mathcal{F}(\xi_{\vec{p}}, \omega_n) = -\frac{\Delta}{\omega_n^2 + \xi_{\vec{p}}^2 + \Delta^2}. \quad (33)$$

We followed Ref. [44] and subtracted from Q_0 in (32) its expression in the normal state, (the second term, with $\mathcal{G}_n(\xi_{\vec{p}}, \omega_n) = 1/(i\omega_n - \xi_{\vec{p}})$), because there is no superconducting current in the normal metal. In this form, the integrand is regular and the integrations over momentum and frequency can be performed in arbitrary order. We

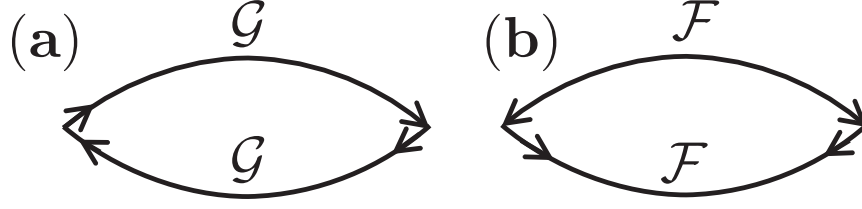


FIG. 3: Diagrammatic representation of the current correlation function in a BCS superconductor. Diagrams (a) and (b) represent normal and anomalous contributions.

integrate (32) over ξ first. The second term then drops out, and in the first we can safely set $\vec{k} = 0$ after the integration. The angular integration yields $\int (d\theta/2\pi) v_{x,\vec{p}}^2 = v_F^2/2 = p_F^2/2m^2$, and Q_0 becomes

$$Q_0 = \frac{e^2}{m^2 c} \frac{p_F^2}{d} N_F \int_0^\infty d\omega_n \frac{\Delta^2}{(\omega_n^2 + \Delta^2)^{3/2}}. \quad (34)$$

Integrating over ω_n we obtain

$$Q_0 = \frac{e^2 n_s}{mc}, \quad n_s = N_F \frac{p_F^2}{md}. \quad (35)$$

Using $N_F = m/(2\pi)$ and the relation between p_F and the full density $n = p_F^2/(2\pi d)$ we find (at $T = 0$) $n_s = n$ and $Q_0 = ne^2/(mc)$ – the textbook result. Alternatively, one could integrate over ω_m first. Then the first term in Eq. (32) vanishes at $T = 0$, while the second one exactly reproduces Eq. (35) with $n = n_s$ (see e.g., Ref. [45]).

We now proceed with the interacting case. We label interaction correction to Q_0 as δQ ($Q = Q_0 + \delta Q$). The total δQ is the sum of self energy and vertex corrections, $\delta Q = \delta Q_\Sigma + \delta Q_V$. At one-loop order, δQ is represented by the three basic diagrams in Fig. 4.

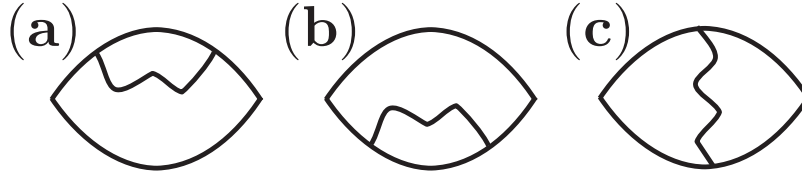


FIG. 4: Diagrammatic representation of the interaction corrections to the current correlation function. Diagrams (a) and (b) represent self energy corrections δQ_Σ , and (c) represents vertex correction δQ_V . The straight lines denote fermion propagators, which can be either normal or anomalous, and the wavy line denotes the boson propagator either in the spin or in the density channel.

Galilean invariant case

We start with the case when the fermion-fermion interaction is restricted to the intra-pocket one and consider a single pocket with a quadratic dispersion. We analyze separately the cases when the intra-pocket interaction is the density and the spin channels.

To account for the overall factors of different diagrams with normal and anomalous Green's functions, it is convenient to treat interaction corrections to Q in the Nambu formalism. We introduce the Nambu spinor $\chi_{\vec{p},\epsilon_n}^{tr} = [\chi_{\vec{p},\epsilon_n}^{(1)}, \chi_{\vec{p},\epsilon_n}^{(2)}] = [\psi_{\uparrow;\vec{p},\epsilon_n}, \psi_{\downarrow;-\vec{p},-\epsilon_n}^\dagger]$. We denote by τ_x, τ_y, τ_z the Pauli matrices operating in Nambu space along with the unit matrix $\tau_0 = 1$. The current operator in Nambu representation is $\vec{j} = e \sum_{\vec{p}} \chi_{\vec{p}}^\dagger \vec{v}_{\vec{p}} \tau_0 \chi_{\vec{p}}$. The non-interacting Nambu Green

function is

$$\hat{G}(\vec{p}, \omega_n) = \frac{i\omega_n \tau_0 + \xi_{\vec{p}} \tau_z + \Delta \tau_x}{\omega_n^2 + \xi_{\vec{p}}^2 + \Delta^2}. \quad (36)$$

The Nambu Green function (36) is related to the normal and anomalous Green functions as

$$\hat{G}(\vec{p}, \omega_n) = \begin{bmatrix} \mathcal{G}(\vec{p}, \omega_n) & -\mathcal{F}(\vec{p}, \omega_n) \\ -\mathcal{F}(\vec{p}, \omega_n) & -\mathcal{G}(-\vec{p}, -\omega_n) \end{bmatrix}. \quad (37)$$

Interaction in the density channel

Consider first the case when the dominant intra-pocket interaction is between fermion densities. Such an interaction is generally described by the effective action $S_{int} = -(1/2) \sum_{\vec{q}, m} L_{\vec{q}, \Omega_m}^\rho \rho_{\vec{q}, \Omega_m} \rho_{-\vec{q}, -\Omega_m}$, where $\rho(\vec{q}, \Omega_m) = T \sum_{\vec{p}, \omega_m, \alpha} \psi_{\vec{p}, \omega_m, \alpha}^\dagger \psi_{\vec{p}+\vec{q}, \omega_m+\Omega_m, \alpha}$ ($\alpha = 1, 2$ accounts for spin). In the Nambu representation, $\rho_{\vec{q}} = \sum_{\vec{p}} \chi_{\vec{p}+\vec{q}}^\dagger \tau_z \chi_{\vec{p}}$. The function $L^\rho(\vec{q}, \Omega_m)$ is an effective propagator of charge fluctuation which in the case of intra-pocket interaction is peaked at $\vec{q} = 0, \Omega_m = 0$ and decreases when each of these two parameters increases.

The self energy correction to the static current correlation function is

$$\delta Q_\Sigma = 2e^2 c^{-1} d^{-1} T \sum_{\vec{p}, \omega_n} T \sum_{\vec{q}, \Omega_m} L^\rho(\vec{q}, \Omega_m) \text{Tr} \left[v_{x, \vec{p}} \hat{G}(\vec{p}, \omega_n) \tau_z \hat{G}(\vec{p} + \vec{q}, \omega_n + \Omega_m) \tau_z \hat{G}(\vec{p}, \omega_n) v_{x, \vec{p}} \hat{G}(\vec{p}, \omega_n) \right], \quad (38)$$

where Tr stands for trace operation in Nambu space, and the factor of 2 accounts for two self-energy diagrams in Fig. 4. Once the trace over the Nambu indices is taken, δQ_Σ can be represented diagrammatically by graphs shown in the first two lines in Fig. 5. Because our primary goal is to understand when vertex and self-energy corrections cancel out and when they add up, we make an additional simplifying assumption that the characteristic momenta and frequency, above which charge propagator $L^\rho(\vec{q}, \Omega_m)$ decreases, are much smaller than Δ/v_F and Δ , respectively. In this situation, the integrations over the fermion and boson energies and momenta separate, and Eq. (38) takes the form

$$\delta Q_\Sigma = e^2 c^{-1} d^{-1} L_0^\rho I_\Sigma, \quad (39)$$

where

$$L_0^\rho = T \sum_{\vec{q}, \Omega_m} L^\rho(\vec{q}, \Omega_m) = L^\rho(\vec{x} = 0, t = 0) \quad (40)$$

is an instantaneous interaction, and

$$I_\Sigma = 2T \sum_{\vec{p}, \omega_n} \text{Tr} \left[v_{\vec{p}, x} \hat{G}(\vec{p}, \omega_n) \tau_z \hat{G}(\vec{p}, \omega_n) \tau_z \hat{G}(\vec{p}, \omega_n) v_{\vec{p}, x} \hat{G}(\vec{p}, \omega_n) \right]. \quad (41)$$

Taking the trace in Eq. (41) with Eq. (37) we obtain explicitly,

$$I_\Sigma = \langle \bar{v}_{\vec{p}}^2 \rangle T \sum_{\vec{p}, \omega_n} [\mathcal{G}^4 + \mathcal{G}_-^4 - 2\mathcal{F}^4], \quad (42)$$

where $\mathcal{G}_-(\vec{p}, \omega_n) = \mathcal{G}(-\vec{p}, -\omega_n)$ and frequency and momenta arguments are omitted for clarity.

For the vertex correction part we obtain, within the same approximation

$$\delta Q_V = e^2 c^{-1} d^{-1} L_0^\rho I_V, \quad (43)$$

where

$$I_V = T \sum_{\vec{p}, \omega_n} \text{Tr} \left[\hat{G}(\vec{p}, \omega_n) v_{\vec{p}, x} \hat{G}(\vec{p}, \omega_n) \tau_z \hat{G}(\vec{p}, \omega_n) v_{\vec{p}, x} \hat{G}(\vec{p}, \omega_n) \tau_z \right]. \quad (44)$$

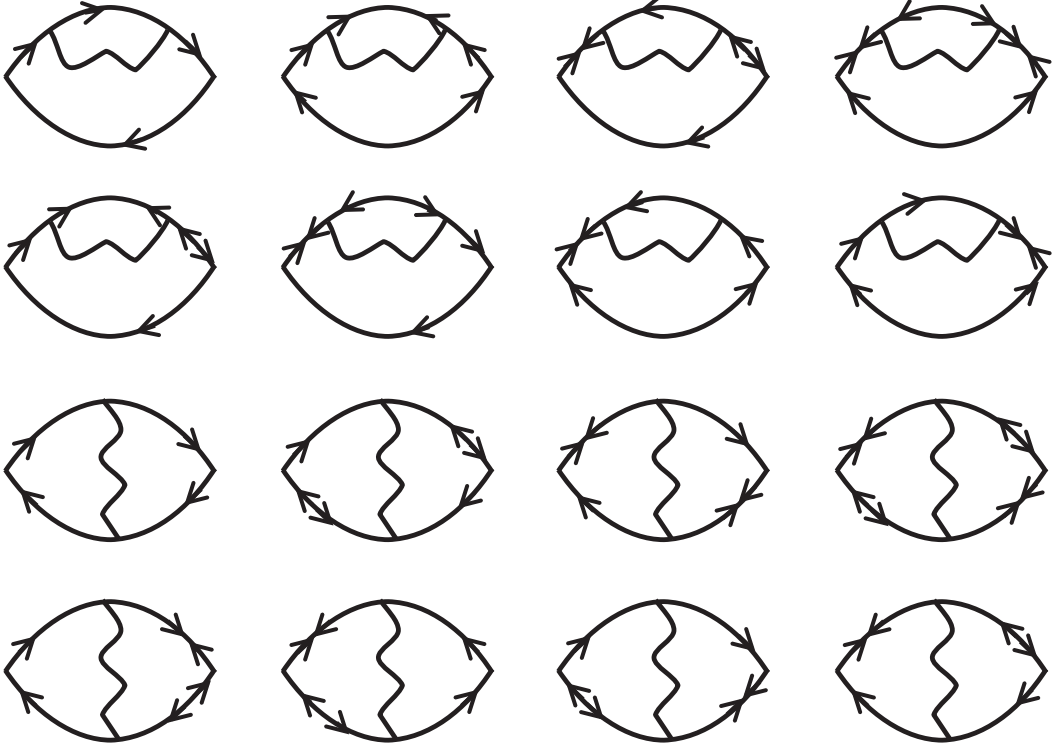


FIG. 5: Diagrammatic representation of the self energy, Eq. (38), (first and second row) and vertex corrections, Eqs. (43), (44) (third and fourth rows). Fermion propagators with a single arrow stand for a normal Green functions, \mathcal{G} . The double arrowed lines designate the anomalous Green functions, \mathcal{F} . These contributions (with the proper signs) are obtained after taking the trace in the expressions for Δ_Q in the Nambu formalism, Eqs. (38) and (44).

Taking again the trace in Nambu space, we obtain the diagrams presented in the last two lines in Fig. 5. Evaluating them, we find

$$I_V = \frac{\langle \bar{v}_{\vec{p}}^2 \rangle}{2} T \sum_{\vec{p}, \omega_n} [\mathcal{G}^4 + \mathcal{G}_-^4 + 2\mathcal{F}^4 + 4\mathcal{F}^2 \mathcal{G} \mathcal{G}_-] . \quad (45)$$

At $T = 0$ the frequency summation is replaced by integration. Evaluating frequency and momentum integrals by, e.g., by using polar coordinates, we obtain

$$T \sum_{\vec{p}, \omega_n} \mathcal{F}^4 = 2T \sum_{\vec{p}, \omega_n} \mathcal{F}^2 \mathcal{G} \mathcal{G}_- = \frac{N_F}{6\Delta^2}, \quad T \sum_{\vec{p}, \omega_n} \mathcal{G}^4 = T \sum_{\vec{p}, \omega_n} \mathcal{G}_-^4 = T \sum_{\vec{p}, \omega_n} \mathcal{F}^2 \mathcal{G}^2 = T \sum_{\vec{p}, \omega_n} \mathcal{F}^2 \mathcal{G}_-^2 = 0 . \quad (46)$$

This gives

$$I_\Sigma = -I_V = \frac{1}{3} \frac{\langle \bar{v}_{\vec{p}}^2 \rangle N_F}{\Delta^2} . \quad (47)$$

We see that self-energy and vertex corrections to the static current correlation function in an s-wave superconductor cancel each other, as it indeed should be the case because of Galilean invariance.

Interaction in the spin channel

We now check that the cancelation in the Galilean invariant case holds also for the case when the intra-pocket interaction in the spin channel. The effective action is now $S_{int} = -(1/2) \sum_{\vec{q}, m} L_{\vec{q}, \Omega_m}^\sigma \vec{\sigma}_{\vec{q}, \Omega_m} \vec{\sigma}_{-\vec{q}, -\Omega_m}$. The Nambu formalism is inconvenient in this case as the spin operator doesn't have a simple form of a product of a Nambu field operator and its conjugate. This formal difficulty can be alleviated by introducing Balian-Werthhammer (BW) [46] extension of the Nambu formalism. The four-dimensional BW spinors are defined as

$$\Psi_{\vec{p}} = [\Psi_{11}, \Psi_{12}, \Psi_{21}, \Psi_{22}]^{tr} = [c_{\vec{p}, \uparrow}, c_{\vec{p}, \downarrow}, -c_{-\vec{p}, \downarrow}^\dagger, c_{-\vec{p}, \uparrow}^\dagger]^{tr}. \quad (48)$$

These spinors form a tensor product of Nambu space and original spin space. Let $\sigma_x, \sigma_y, \sigma_z$ be spin Pauli matrices, and σ_0 the unit matrix. The current, density, and spin density operators are $\rho = (1/2) \sum_{\vec{p}} \Psi_{\vec{p}}^\dagger \tilde{\rho} \Psi_{\vec{p}}$, $\vec{j} = e\vec{v}$, $\vec{v} = (1/2) \sum_{\vec{p}} \Psi_{\vec{p}}^\dagger \tilde{\vec{v}} \Psi_{\vec{p}}$ and $\vec{\sigma} = (1/2) \sum_{\vec{p}} \Psi_{\vec{p}}^\dagger \tilde{\vec{\sigma}} \Psi_{\vec{p}}$, where

$$\tilde{\rho}_{\vec{p}} = \tau_z \otimes \sigma_0, \quad \tilde{\vec{v}}_{\vec{p}} = \vec{v}_{\vec{p}} \tau_0 \otimes \sigma_0, \quad \tilde{\vec{\sigma}} = \tau_0 \otimes \sigma, \quad (49)$$

and \otimes stands for a tensor product. The Green function in BW space is expressed via the Nambu Green function, Eq. (36), as

$$\check{G} = \hat{G} \otimes \sigma_0. \quad (50)$$

The main advantage of the BW formalism is that it allows one to use standard diagrammatic rules, including (-1) rule for each closed loop.

We found that Eqs (39), (40), and (43) preserve their form, with L^σ instead of L^ρ , but Eqs. (41) and (44) become, respectively

$$I_\Sigma = T \sum_{\vec{p}, \omega_n} \text{Tr} [\check{V}_{\vec{p}, x} \check{G}(\vec{p}, \omega_n) \tilde{\vec{\sigma}} \check{G}(\vec{p}, \omega_n) \tilde{\vec{\sigma}} \check{G}(\vec{p}, \omega_n) \check{V}_{\vec{p}, x} \check{G}(\vec{p}, \omega_n)] \quad (51)$$

and

$$I_V = \frac{1}{2} T \sum_{\vec{p}, \omega_n} \text{Tr} [\check{G}(\vec{p}, \omega_n) \check{V}_{\vec{p}, x} \check{G}(\vec{p}, \omega_n) \tilde{\vec{\sigma}} \check{G}(\vec{p}, \omega_n) \check{V}_{\vec{p}, x} \check{G}(\vec{p}, \omega_n) \tilde{\vec{\sigma}}]. \quad (52)$$

An extra factor of 1/2 as compared to (41) and (44) compensates for the double counting of degrees of freedom in BW formalism. Taking the trace in (51) and (52) we obtain

$$I_\Sigma = 3 \langle \tilde{v}_{\vec{p}}^2 \rangle T \sum_{\vec{p}, \omega_n} [2\mathcal{F}^4 + 4\mathcal{F}^2 (\mathcal{G}^2 - \mathcal{G}\mathcal{G}_- + \mathcal{G}_-^2) + \mathcal{G}^4 + \mathcal{G}_-^4], \quad (53)$$

$$I_V = 3 \frac{\langle \tilde{v}_{\vec{p}}^2 \rangle}{2} T \sum_{\vec{p}, \omega_n} [2\mathcal{F}^4 + 4\mathcal{F}^2 (\mathcal{G}^2 - \mathcal{G}\mathcal{G}_- + \mathcal{G}_-^2) + \mathcal{G}^4 + \mathcal{G}_-^4] \quad (54)$$

respectively. Using Eq. (46) we immediately find that

$$I_\Sigma = I_V = 0, \quad (55)$$

i.e., self energy and vertex corrections simply vanish.

The case of inter-pocket interaction

The basic formalism set up in the previous subsection can be applied to the case when the interactions $L^{\rho, \sigma}(\vec{q}, \Omega_m)$ are peaked at large momentum $\vec{q} = \vec{Q}$, and couple hole and electron pockets. We consider the simplest situation of perfect nesting, when the electron and the hole dispersions are $\xi_{\vec{p}}^e = -\xi_{\vec{p}+\vec{Q}}^h = \xi_{\vec{p}}$. In this case, the velocity of a fermions at a point \mathbf{k} on the hole pocket is opposite to that of a fermion at $\mathbf{k} + \mathbf{Q}$ on the electron pocket. We also assume that $\Delta_e = -\Delta_h = \Delta$. Finally, like in the previous case, we assume that $L^{\rho, \sigma}(\vec{q}, \Omega_m)$ are rapidly decaying functions of $\vec{q} - \vec{Q}$ and Ω_m , and that characteristic $\vec{q} - \vec{Q}$ and Ω_m much smaller than Δ/v_F and Δ , respectively. This again allows us to factorize the integrations over fermion energies and momenta and over boson energy and momentum.

Interaction in the density channel

The electron and hole Nambu Green functions are

$$\hat{G}^{e,h}(\vec{p}, \omega_n) = \frac{i\omega_n\tau_0 \pm \xi_{\vec{p}}\tau_z \pm \Delta\tau_x}{\omega_n^2 + \xi_{\vec{p}}^2 + \Delta^2}. \quad (56)$$

Equation (39) should be modified to include both hole and electron pockets and becomes

$$\delta Q_{\Sigma} = \frac{e^2}{dc} L_{\pi}^{\rho} (I_{\Sigma}^e + I_{\Sigma}^h), \quad (57)$$

where

$$L_{\pi}^{\rho} = T \sum_{\vec{q} \approx \vec{Q}, \Omega_m} L^{\rho}(\vec{q}, \Omega_m) \quad (58)$$

and

$$I_{\Sigma}^{e(h)} = 2T \sum_{\vec{p}, \omega_n} \text{Tr} \left[v_{\vec{p},x}^{e(h)} \hat{G}^{e(h)}(\vec{p}, \omega_n) \tau_z \hat{G}^{h(e)}(\vec{p}, \omega_n) \tau_z \hat{G}^{e(h)}(\vec{p}, \omega_n) v_{\vec{p},x}^{e(h)} \hat{G}^{e(h)}(\vec{p}, \omega_n) \right]. \quad (59)$$

Taking the trace and counting pre-factors, we obtain

$$\begin{aligned} I_{\Sigma}^e = I_{\Sigma}^h = \langle \vec{v}_{\vec{p}}^2 \rangle T \sum_{\vec{p}, \omega_n} & \left[-2\mathcal{F}_e^3 \mathcal{F}_h + \mathcal{F}_e^2 (2\mathcal{G}_e \mathcal{G}_h - \mathcal{G}_e \mathcal{G}_{h,-} - \mathcal{G}_{e,-} \mathcal{G}_h + 2\mathcal{G}_{e,-} \mathcal{G}_{h,-}) \right. \\ & \left. - 2\mathcal{F}_e \mathcal{F}_h (\mathcal{G}_e^2 - \mathcal{G}_e \mathcal{G}_{e,-} + \mathcal{G}_{e,-}^2) + \mathcal{G}_e^3 \mathcal{G}_h + \mathcal{G}_{e,-}^3 \mathcal{G}_{h,-} \right]. \end{aligned} \quad (60)$$

The non-zero contributions are

$$T \sum_{\vec{p}, \omega_n} \mathcal{F}_e^3 \mathcal{F}_h = 2T \sum_{\vec{p}, \omega_n} \mathcal{F}_e^2 \mathcal{G}_e \mathcal{G}_h = 2T \sum_{\vec{p}, \omega_n} \mathcal{F}_e^2 \mathcal{G}_{e,-} \mathcal{G}_{h,-} = 2T \sum_{\vec{p}, \omega_n} \mathcal{F}_e \mathcal{F}_h \mathcal{G}_e \mathcal{G}_{e,-} = -\frac{N_F}{6\Delta^2}. \quad (61)$$

Substituting this into (60), we obtain

$$I_{\Sigma}^e = I_{\Sigma}^h = I_V^{eh} = I_V^{he} = -\frac{1}{6} \frac{\langle \vec{v}_{\vec{p}}^2 \rangle N_F}{\Delta^2}. \quad (62)$$

The vertex correction contribution so the current-current correlation function is

$$\delta Q_V = \frac{e^2}{cd} L_{\pi}^{\rho} (I_V^{eh} + I_V^{he}), \quad (63)$$

where now

$$I_V^{eh(he)} = T \sum_{\vec{p}, \omega_n} \text{Tr} \left[\hat{G}^{e(h)}(\vec{p}, \omega_n) v_{\vec{p},x}^{e(h)} \hat{G}^{e(h)}(\vec{p}, \omega_n) \tau_z \hat{G}^{h(e)}(\vec{p}, \omega_n) v_{\vec{p},x}^{h(e)} \hat{G}^{h(e)}(\vec{p}, \omega_n) \tau_z \right]. \quad (64)$$

After taking the trace, this becomes

$$\begin{aligned} I_V^{eh} = I_V^{he} = -\frac{\langle \vec{v}_{\vec{p}}^2 \rangle}{2} T \sum_{\vec{p}, \omega_n} & \left[\mathcal{G}_e^2 \mathcal{G}_h^2 + \mathcal{G}_{e,-}^2 \mathcal{G}_{h,-}^2 + 2\mathcal{F}_e^2 \mathcal{F}_h^2 + \mathcal{F}_h^2 (\mathcal{G}_e^2 + \mathcal{G}_{e,-}^2) + \mathcal{F}_e^2 (\mathcal{G}_h^2 + \mathcal{G}_{h,-}^2) \right. \\ & \left. - 2\mathcal{F}_h \mathcal{F}_e (\mathcal{G}_e \mathcal{G}_h + \mathcal{G}_{e,-} \mathcal{G}_{h,-} - \mathcal{G}_{e,-} \mathcal{G}_h - \mathcal{G}_e \mathcal{G}_{h,-}) \right]. \end{aligned} \quad (65)$$

The non-zero terms in (65) are

$$T \sum_{\vec{p}, \omega_n} \mathcal{G}_e^2 \mathcal{G}_h^2 = T \sum_{\vec{p}, \omega_n} \mathcal{G}_{e,-}^2 \mathcal{G}_{h,-}^2 = T \sum_{\vec{p}, \omega_n} \mathcal{F}_e^2 \mathcal{F}_h^2 = 2T \sum_{\vec{p}, \omega_n} \mathcal{F}_h \mathcal{F}_e \mathcal{G}_e \mathcal{G}_h = 2T \sum_{\vec{p}, \omega_n} \mathcal{F}_h \mathcal{F}_e \mathcal{G}_{e,-} \mathcal{G}_{h,-} = \frac{N_F}{6\Delta^2}. \quad (66)$$

Substituting into (65), we obtain

$$I_V^{eh} = I_V^{he} = -\frac{1}{6} \frac{\langle \vec{v}_{\vec{p}}^2 \rangle N_F}{\Delta^2}. \quad (67)$$

Evidently, $\delta Q_\Sigma = \delta Q_V$, i.e., self-energy and vertex corrections add up rather than cancel out. By obvious reasons, non-cancellation survives even if we relax the assumption of a perfect nesting and of exactly opposite values of the gaps on hole and electron pockets, and do not require that $L^{\rho,\sigma}(\vec{q}, \Omega_m)$ are rapidly decaying functions of $\vec{q} - \vec{Q}$ and Ω_m .

The total $\delta Q = \delta Q_\Sigma + \delta Q_V$ is

$$\delta Q = -\frac{2}{3} \frac{e^2}{dc} L_\pi^\rho \frac{\langle \vec{v}_{\vec{p}}^2 \rangle N_F}{\Delta^2}. \quad (68)$$

The relative correction to the penetration depth

$$\frac{\delta \lambda}{\lambda_0} = -\frac{\delta Q}{2Q_0} = \frac{L_\pi^\rho}{6\Delta^2}, \quad (69)$$

where Q_0 is given by Eq. (35), and the factor of 2 is because we include both electron and hole pockets. We see that the corrections tend to increase the penetration depth. The instantaneous interaction L_π^ρ , given by Eq. (40), is of order $H_{int} t_{ret}^{-1}$, where H_{int} is the typical local interaction strength, and t_{ret} is the retardation time. Equation (69) shows that the perturbation theory is valid provided, $H_{int} \ll \Delta(t_{ret} \Delta)$. Because we assumed $t_{ret} \gg \Delta^{-1}$, the perturbative approach is valid even if the interaction exceeds Δ .

Interaction in the spin channel

Consider next inter-pocket interaction in the spin channel. Applying the BW formalism, we obtain, after straightforward calculations

$$I_\Sigma^{e(h)} = T \sum_{\vec{p}, \omega_n} \text{Tr} \left[\check{V}_{\vec{p},x}^{e(h)} \check{G}^{e(h)}(\vec{p}, \omega_n) \check{\sigma} \check{G}^{h(e)}(\vec{p}, \omega_n) \check{\sigma} \check{G}^{e(h)}(\vec{p}, \omega_n) \check{V}_{\vec{p},x}^{e(h)} \check{G}^{e(h)}(\vec{p}, \omega_n) \right], \quad (70)$$

and

$$I_V^{e(h)e} = \frac{1}{2} T \sum_{\vec{p}, \omega_n} \text{Tr} \left[\check{G}^{e(h)}(\vec{p}, \omega_n) \check{V}_{\vec{p},x}^{e(h)} \check{G}^{e(h)}(\vec{p}, \omega_n) \check{\sigma} \check{G}^{h(e)}(\vec{p}, \omega_n) \check{V}_{\vec{p},x}^{(h)e} \check{G}^{(h)e}(\vec{p}, \omega_n) \check{\sigma} \right]. \quad (71)$$

Taking the trace over spin and Nambu indices we get

$$I_\Sigma^e = I_\Sigma^h = 3 \langle \vec{v}_{\vec{p}}^2 \rangle T \sum_{\vec{p}, \omega_n} \left[2\mathcal{F}_e^3 \mathcal{F}_h + 2\mathcal{F}_e \mathcal{F}_h (\mathcal{G}_e^2 - \mathcal{G}_e \mathcal{G}_{e,-} + \mathcal{G}_{e,-}^2) + \mathcal{G}_e^3 \mathcal{G}_h + \mathcal{G}_{e,-}^3 \mathcal{G}_{h,-} + \mathcal{F}_e^2 (2\mathcal{G}_e \mathcal{G}_h - \mathcal{G}_{e,-} \mathcal{G}_h - \mathcal{G}_e \mathcal{G}_{h,-} + 2\mathcal{G}_{e,-} \mathcal{G}_{h,-}) \right], \quad (72)$$

$$I_V^{eh} = I_V^{he} = -3 \frac{\langle \vec{v}_{\vec{p}}^2 \rangle}{2} T \sum_{\vec{p}, \omega_n} \left[\mathcal{F}_h^2 (\mathcal{G}_e^2 + \mathcal{G}_{e,-}^2) + \mathcal{G}_e^2 \mathcal{G}_h^2 + 2\mathcal{F}_e \mathcal{F}_h (\mathcal{G}_e \mathcal{G}_h + \mathcal{G}_{e,-} \mathcal{G}_{h,-} - \mathcal{G}_{e,-} \mathcal{G}_h - \mathcal{G}_e \mathcal{G}_{h,-}) + \mathcal{G}_{e,-}^2 \mathcal{G}_{h,-}^2 + \mathcal{F}_e^2 (2\mathcal{F}_h^2 + \mathcal{G}_h^2 + \mathcal{G}_{h,-}^2) \right] \quad (73)$$

The non-zero terms in Eqs. (72) and (73) are listed in Eqs. (61) and (66). Substituting them, we obtain

$$I_\Sigma^e = I_\Sigma^h = I_V^{eh} = I_V^{he} = -3 \frac{\langle \vec{v}_{\vec{p}}^2 \rangle N_F}{2\Delta^2}. \quad (74)$$

We see that self-energy and vertex corrections again add up. Combining the two, we obtain

$$\delta Q = -6 \frac{e^2}{dc} L_\pi^\sigma \frac{\langle \vec{v}_{\vec{p}}^2 \rangle N_F}{\Delta^2}. \quad (75)$$

The correction to the penetration depth is

$$\frac{\delta \lambda}{\lambda_0} = -\frac{\delta Q}{2Q_0} = \frac{3L_\pi^\sigma}{2\Delta^2}. \quad (76)$$

In the calculations of the current correlation function in the normal state, it is important to include into consideration also Aslamazov-Larkin diagrams [47], which contain two boson propagators L coupled via two triangular fermionic vertex blocks. We analyzed these diagrams for our case and found that they are irrelevant. First, for the case when the gaps on hole and electron FSs are of equal magnitude (and opposite sign), there is a cancelation of the dominant Aslamazov-Larkin terms. The cancelation occurs at the level of the valuation of the fermionic triangular vertex – for each block there are two ways to arrange electron and hole Green’s function lines and their corresponding momenta which cancel each other. For non-equal gap magnitudes, the cancelation is not perfect. Still, even in this case, the Aslamazov-Larkin terms can be safely neglected. The reason is the following: the overall factor in Aslamazov-Larkin terms contains two additional powers of the coupling constant. In the normal state, these two additional powers are eliminated by the need to regularize the divergence coming out of integration of the two bosonic propagators. In the superconducting state, the corresponding integral is finite because for small q each triangular block scales as $v_F q / \Delta$. As a result, the two extra powers of the coupling do not cancel.

-
- [1] Y. Kamihara, T. Watanabe, M. Hirano, and H. Hosono, *J. Am. Chem. Soc.* **130**, 3296 (2008).
 - [2] X. H. Chen, T. Wu, G. Wu, R. H. Liu, H. Chen, and D. F. Fang, *Nature (London)* **453**, 761 (2008).
 - [3] G. F. Chen, Z. Li, D. Wu, G. Li, W. Z. Hu, J. Dong, P. Zheng, J. L. Luo, and N. L. Wang, *Phys. Rev. Lett.* **100**, 247002 (2008).
 - [4] M. Rotter, M. Tegel, and D. Johrendt, *Phys. Rev. Lett.* **101**, 107006 (2008).
 - [5] H. Luetkens, H.-H. Klauss, M. Kraken, F. J. Litterst, T. Dellmann, R. Klingeler, C. Hess, R. Khasanov, A. Amato, C. Baines, M. Kosmala, O. J. Schumann, M. Braden, J. Hamann-Borrero, N. Leps, A. Kondrat, G. Behr, J. Werner, and B. Büchner, *Nature Mater.* **8**, 305 (2009).
 - [6] A. J. Drew, Ch. Niedermayer, P. J. Baker, F. L. Pratt, S. J. Blundell, T. Lancaster, R. H. Liu, G. Wu, X. H. Chen, I. Watanabe, V. K. Malik, A. Dubroka, M. Rössle, K. W. Kim, C. Baines, and C. Bernhard, *Nature Mater.* **8**, 310 (2009).
 - [7] N. Ni, M. E. Tillman, J.-Q. Yan, A. Kracher, S. T. Hannahs, S. L. Bud’ko, and P. C. Canfield, *Phys. Rev. B* **78**, 214515 (2008).
 - [8] J.-H. Chu, J. G. Analytis, C. Kucharczyk, and I. R. Fisher, *Phys. Rev. B* **79**, 014506 (2009).
 - [9] see, e.g., P. J. Hirschfeld, M. M. Korshunov, and I. I. Mazin, *Rep. Prog. Phys.* **74**, 124508 (2011); A. V. Chubukov, *Annul. Rev. Cond. Mat. Phys.* **3**, 13.113.36, (2012) and references therein.
 - [10] S. Nandi, M. G. Kim, A. Kreyssig, R. M. Fernandes, D. K. Pratt, A. Thaler, N. Ni, S. L. Budko, P. C. Canfield, J. Schmalian, R. J. McQueeney, and A. I. Goldman, *Phys. Rev. Lett.* **104**, 057006 (2010).
 - [11] see e.g. E. G. Moon and S. Sachdev, *Phys. Rev. B* **78**, 184509 (2008).
 - [12] R. M. Fernandes and J. Schmalian, *Phys. Rev. B* **82**, 014521 (2010).
 - [13] M. G. Vavilov, A. V. Chubukov, and A. B. Vorontsov, *Supercond. Sci. Technol.* **23**, 054011 (2010).
 - [14] A. B. Vorontsov, M. G. Vavilov, and A. V. Chubukov, *Phys. Rev. B* **81**, 174538 (2010).
 - [15] Y. Laplace, J. Bobroff, F. Rullier-Albenque, D. Colson, and A. Forget, *Phys. Rev. B* **80**, 140501(R) (2009).
 - [16] M.-H. Julien, H. Mayaffre, M. Horvatic, C. Berthier, X. D. Zhang, W. Wu, G. F. Chen, N. L. Wang, and J. L. Luo, *EPL* **87**, 37001 (2009).
 - [17] C. Bernhard, A. J. Drew, L. Schulz, V. K. Malik, M. Rössle, C. Niedermayer, T. Wolf, G. D. Varma, G. Mu, H. H. Wen, H. Liu, G. Wu, and X. H. Chen, *New J. Phys.* **11**, 055050 (2009).
 - [18] F. Ning, K. Ahilan, T. Imai, A. S. Sefat, R. Jin, M. A. McGuire, B. C. Sales, and D. Mandrus, *J. Phys. Soc. Jpn.* **78**, 013711 (2009).
 - [19] C. Lester, J.-H. Chu, J. G. Analytis, S. C. Capelli, A. S. Erickson, C. L. Condon, M. F. Toney, I. R. Fisher, and S. M. Hayden, *Phys. Rev. B* **79**, 144523 (2009).
 - [20] D. K. Pratt, W. Tian, A. Kreyssig, J. L. Zarestky, S. Nandi, N. Ni, S. L. Bud’ko, P. C. Canfield, A. I. Goldman, and R. J. McQueeney, *Phys. Rev. Lett.* **103**, 087001 (2009).
 - [21] H. Chen, Y. Ren, Y. Qiu, W. Bao, R. H. Liu, G. Wu, T. Wu, Y. L. Xie, X. F. Wang, Q. Huang, and X. H. Chen, *EPL* **85**, 17006 (2009).
 - [22] M. Rotter, M. Tegel, I. Schellenberg, F. M. Schappacher, R. Pöttgen, J. Deisenhofer, A. Günther, F. Schrettle, A. Loidl, and D. Johrendt, *New J. Phys.* **11**, 025014 (2009).
 - [23] Z. Li, R. Zhou, Y. Liu, D. L. Sun, J. Yang, C. T. Lin, and Guo-qing Zheng, *Phys. Rev. B* **86**, 180501(R) (2012).
 - [24] A. Blachowski, K. Ruebenbauer, J. Zukrowski, Z. Bukowski, K. Rogacki, P. J. W. Moll, and J. Karpinski, *Phys. Rev. B* **84**, 174503 (2011).
 - [25] H. Shishido, A. Bangura, A. Coldea, S. Tonegawa, K. Hashimoto, S. Kasahara, P. Rourke, H. Ikeda, T. Terashima, R. Settai, Y. Onuki, D. Vignolles, C. Proust, B. Vignolle, A. Mccollam, Y. Matsuda, T. Shibauchi, and A. Carrington, *Phys. Rev. Lett.* **104**, 057008 (2010).
 - [26] K. Hashimoto, K. Cho, T. Shibauchi, S. Kasahara, Y. Mizukami, R. Katsumata, Y. Tsuruhara, T. Terashima, H. Ikeda,

- M. A. Tanatar, H. Kitano, N. Salovich, R. W. Giannetta, P. Walmsley, A. Carrington, R. Prozorov, Y. Matsuda, *Science* **336**, 1554 (2012).
- [27] A. Abanov, A. V. Chubukov, and J. Schmalian, *Adv. Phys.*, **52**, 119 (2003); H. Meier, C. Pepin and K. B. Efetov, arXiv:1210.3276.
- [28] M. A. Metlitski and S. Sachdev, *Phys. Rev. B* **82**, 075128 (2010).
- [29] A. Pelissetto, S. Sachdev, and E. Vicari, *Phys. Rev. Lett.*, **101**, 027005 (2008).
- [30] R. T. Gordon, H. Kim, N. Salovich, R. W. Giannetta, R. M. Fernandes, V. G. Kogan, T. Prozorov, S. L. Bud'ko, P. C. Canfield, M. A. Tanatar, and R. Prozorov, *Phys. Rev. B* **82**, 054507 (2010).
- [31] see, e.g., S. Kasahara, T. Shibauchi, K. Hashimoto, K. Ikada, S. Tonegawa R. Okazaki, H. Shishido, H. Ikeda, H. Takeya, K. Hirata, T. Terashima, and Y. Matsuda, *Phys. Rev. B* **81**, 184519, (2010).
- [32] R. M. Fernandes, A. V. Chubukov, J. Knolle, I. Eremin, and J. Schmalian, *Phys. Rev. B* **85**, 024534 (2012).
- [33] M. G. Vavilov, A. V. Chubukov, and A. B. Vorontsov, *Phys. Rev. B* **84**, 140502(R) (2011).
- [34] D. Kuzmanovski and M. G. Vavilov, *Supercond. Sci. Technol.* **25**, 084001 (2012).
- [35] A. I. Larkin, *Sov. Phys. JETP* **19**, 1478 (1964).
- [36] A. J. Leggett, *Phys. Rev.* **140**, A1869 (1965).
- [37] See Supplementary material for details.
- [38] C. M. Varma, K. Miyake, and S. Schmitt-Rink, *Phys. Rev. Lett.* **57**, 626 (1986).
- [39] S. A. Hartnoll, D. M. Hofman, M. A. Metlitski, and S. Sachdev, *Phys. Rev. B* **84**, 125115 (2011).
- [40] Graser, T. A. Maier, P. J. Hirshfeld, D. J. Scalapino, *New J. Phys.* **11**, 025016 (2009).
- [41] A. V. Chubukov, D. Efremov, and I. Eremin, *Phys. Rev. B* **78**, 134512 (2008); A. V. Chubukov *Physica C* **469**, 640(2009).
- [42] A. Abanov, A. V. Chubukov, and J. Schmalian, *Adv. Phys.*, **52**, 119 (2003).
- [43] Y. B. Kim, A. Furusaki, X-G. Wen, and P. A. Lee, *Phys. Rev.* **50**, 17917 (1994).
- [44] L. P. Pitaevskii, E. M. Lifshitz, *Statistical Physics, Part 2*, (Course of Theoretical Physics Vol. 9), Elsevier (2010).
- [45] J. R. Schrieffer, *Theory of superconductivity*, W. A. Benjamin, Inc., Publishers (1964).
- [46] R. Balian and N. R. Werthammer, *Phys. Rev.* **131**, 1553 (1963).
- [47] A. I. Larkin and A. Varlamov, *Theory of Fluctuations in Superconductors*, (Clarendon Press, Oxford, 2005).